



International Conference on Computational Science, ICCS 2013

## Performance Analysis of Two Quantum Reaction Dynamics Codes: Time-Dependent and Time-Independent Strategies

Pablo Gamallo<sup>a</sup>, Miguel González, and Fermín Huarte-Larrañaga<sup>b</sup>

*Departament de Química Física and IQTCUB, Universitat de Barcelona, Martí i Franqués 1, Barcelona 08028, Spain*

---

### Abstract

The computer simulation of reaction dynamics has nowadays reached a remarkable degree of accuracy. Triatomic elementary reactions are rigorously studied with great detail on a straightforward basis using a considerable variety of Quantum Dynamics computational tools available to the scientific community. In our contribution we compare the performance of two quantum scattering codes in the computation of reaction cross sections of a triatomic benchmark reaction such as the gas phase reaction  $\text{Ne} + \text{H}_2^+ \rightarrow \text{NeH}^+ + \text{H}$ . The computational codes are selected as representative of time-dependent (Real Wave Packet [1]) and time-independent (ABC [2]) methodologies. The main conclusion to be drawn from our study is that both strategies are, to a great extent, not competing but rather complementary. While time-dependent calculations advantages with respect to the energy range that can be covered in a single simulation, time-independent approaches offer much more detailed information from each single energy calculation. Further details such as the calculation of reactivity at very low collision energies or the computational effort related to account for the Coriolis couplings are analyzed in this paper.

Keywords: Reaction Dynamics, Time-Dependent Dynamics, Time-Independent Dynamics, Quantum Scattering, Wave packets

---

### 1. Introduction

Chemical reaction dynamics is the microscopic basis of chemical reaction kinetics and quantum mechanics determines their evolution at the fundamental level. According to this, the development of theoretical methods as well as the implementation of the corresponding computational tools is a key element for obtaining detailed dynamical information (i.e., cross sections, product state distributions, differential cross sections, rate constants, characterization of the microscopic mechanism, ...) that enable the understanding of elementary chemical reactions from the microscopic point of view [3].

Reaction Dynamics has contributed significantly to the progress of physical chemistry and chemical physics during last decades, especially after 1980s, thanks to the development of many new experimental and theoretical techniques that have provided important support for atmospheric, astrophysical as well as combustion chemistry [4]. At the same time, advances in computer technology and quantum dynamics methods have allowed new possibilities

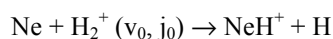
---

<sup>a</sup> [gamallo@ub.edu](mailto:gamallo@ub.edu)

<sup>b</sup> [fermin.huarte@ub.edu](mailto:fermin.huarte@ub.edu)

for theoretical studies. The arrival of competitive *ab initio* quantum chemistry packages became an important tool for obtaining accurate energies as well as structural information. Thus, accurate *ab initio* based global potential energy surfaces (PESs) may now be constructed for elementary reactions and used in reaction dynamics studies. The Schrödinger equation characterizing the rearrangement evolution of the atomic nuclei over PES can be solved using time-dependent (TD) or time-independent (TI) methods. In either case, solving the Schrödinger equation is a formidable task, and many interesting chemical systems challenge the present capabilities of exact quantum dynamics techniques.

In this context, our contribution presents the comparison of two computational codes based on TD and TI quantum scattering methods in the study of a gas-phase atom + diatom reaction. In particular, we have studied the collision dynamics of the benchmark reaction,



for a set of selected rovibrational initial states of the diatomic  $\text{H}_2^+$  ( $v_0=0-2$ ,  $j_0=1$ ) molecule on the recent accurate LZHH PES [5]. The dynamics of this reaction has been investigated in the past by some of us [6, 7, 8] either using the LZHH or an older PES [9]. The reactivity of this system exhibits a strong oscillatory behavior as a function of the collision energy ( $E_{\text{col}}$ ) independently of the PES used.

Our contribution focuses on the computational aspects of both quantum dynamics studies, analyzing the computer time consumed to obtain initial-state resolved reaction probabilities and cross sections. In order to compare TD and TI strategies we have chosen two representative programs. In particular, we employ a parallel version of the time-dependent real wave packet (TDRWP) method of Gray and Balint-Kurti [1] and the time-independent ABC quantum scattering code developed by Skouteris, Castillo, and Manolopoulos [2]. In Section 2 we briefly present both approaches, paying more attention to practical implementation aspects rather than formal derivations. The results obtained in the quantum dynamics studies are commented in Section 3 together with the associated computer resources employed. Our main conclusions are listed in Section 4.

## 2. Methodology

Both quantum methods solve exactly the same equations although some differences appear depending on the set of coordinates that is chosen to solve the problem. The body fixed (BF) Hamiltonian for a triatomic system is widely developed in Ref. [10] in Jacobi coordinates and in Ref. [11] in hyperspherical coordinates. It is composed by the radial and the angular kinetic energy term, the potential energy surface term, the centrifugal energy term (associated with the value of the total angular momentum  $J$ ) and the Coriolis term (associated with the value of  $K$ , the projection of  $J$ ). Since the Coriolis term is considered accurately (i.e., using coupled channel (CC) equations), the dynamics of the system couples the different  $K$  values.

### 2.1. Time-Independent ABC method

The ABC time-independent quantum scattering program<sup>a</sup> [2] integrates the Schrödinger equation for an atom-diatom elementary reaction using the CC method [11]. The program makes use of a TI method to integrate the nuclear Schrödinger equation on a single potential energy surface (PES), within the framework of the Born-Oppenheimer approach. The nuclear wave function,  $\psi$ , is expanded in terms of the hyperspherical arrangement

<sup>a</sup> Available at <http://www.ccp6.ac.uk>

channel  $\alpha$  basis functions  $B_{\alpha v_{\alpha} j_{\alpha} K_{\alpha}}^{JM}$  with  $J$  being the total angular momentum quantum number,  $M$  and  $K_{\alpha}$  the space- and BF projections of  $J$ , respectively, and  $v_{\alpha}$ ,  $j_{\alpha}$  the asymptotic vibrational and rotational quantum numbers. The quantum reactive scattering boundary conditions are applied exactly, without the use of an imaginary absorbing potential [12], and taking also into account the coupling between the initial and final orbital and rotational angular momenta implemented rigorously for each value of  $J$ .

To integrate the set of coupled differential equations the propagation along the hyperradius is divided into various sectors with a constant- $\rho$  reference potential. In each sector, local bound state functions are obtained by diagonalizing the (fixed  $\rho$ ) Hamiltonian. The CC equations are integrated starting from small values of  $\rho$  (by propagating within each sector and chaining adjacent sectors propagations) to the asymptotes where the solutions are matched to the product states. Given that the total angular momentum is a constant of motion and the triatomic parity ( $\sigma$ ) is conserved, the optimal choice to run a complete quantum scattering calculation using ABC is to launch independent runs of ABC program for specified values of  $(J, \sigma)$ . In the case of a diatomic homonuclear molecule, calculations can also be run independently for even ( $p=+1$ ) and odd ( $p=-1$ ) rotational states, optimizing the computational effort in the rotational basis. Each  $(J, \sigma, p)$  set therefore requires a different calculation.

The execution of a single ABC calculation consists of the following tasks:

- A. Determination of the basis set. In each sector, the one-dimensional Schrödinger equation associated with the reference potential in each arrangement channel is solved employing a finite difference method, obtaining vibrational functions. These potentials are usually chosen along fixed hyperangle ( $\Theta_{\alpha}$ ) cuts of the full potential for a  $\rho$  value chosen at the midpoint of the sector. However, to obtain an efficient convergence of the solution it is important pay attention to overcompleteness issues.
- B. Construction of overlap and coupling matrices between adjacent sectors. The most time consuming integrals involve interchannel ( $\alpha \neq \alpha'$ ) matrix elements, this is usually the most time-consuming part of the calculation.
- C. The coupled equation set is solved using the constant reference potential log derivative method [13].
- D. Matching from hyperspherical ( $\rho_{\alpha}, \chi_{\alpha}, \theta_{\alpha}$ ) to Jacobi coordinates ( $R_{\alpha}, r_{\alpha}, \theta_{\alpha}$ ) being  $R_{\alpha}$  the distance from the atom to the molecule center of mass,  $r_{\alpha}$  the internuclear molecular distance and  $\theta_{\alpha}$  the angle between both distances. A substantial saving in computer time is gained by this switch as the propagation moves away from the strong interaction region.
- E. Asymptotic analysis. Once the Jacobi coordinate solutions have been integrated to the asymptotic region ( $R_{\alpha}$  is large enough to consider the potential constant), the scattering matrix can be evaluated by applying the usual scattering boundary conditions [14].

The resulting output files contain parity-adapted scattering matrix elements of the form  $S_{\alpha' v' j' K' \alpha v j K}^{J\sigma}(E)$  where  $\alpha$  and  $\alpha'$  are arrangement labels,  $(v', j')$  and  $(v, j)$  are rovibrational quantum numbers of products and reactants, respectively. Finally  $K$  and  $K'$  are helicity (intermolecular axis angular momentum projection) quantum numbers. In order to compute observables the parity-adapted S-matrix needs to be converted into the standard helicity-representation. Several observable properties can be constructed out of the S-matrix, such as state-to-state probabilities (square modulus of the S-matrix element). However, more useful information can be obtained by considering multiple values of the total angular momentum and calculating properties such as integral or differential cross section for a given range of energies. This means that ABC calculations need to be run for all  $J$  values between 0 and a given  $J_{\max}$ . The fact that these  $(J, \sigma)$ , -independent calculations can be distributed over a high throughput-computing infrastructure is a key factor for the study of relevant reactive processes.

## 2.2. Time-Dependent Real Wave Packet (TDRWP) Method

In the TD quantum dynamics applications an initial wave packet (WP) is set up in a given set of coordinates, propagated in time by solving the TD Schrödinger equation and analyzed to extract relevant dynamical quantities. The WP approach differs from the TI scattering one in the fact that a single propagation generally does not yield information about all possible transitions, but rather about certain specific ones. Such information is, however, obtained over a range of energies. The method used in this work is the time-dependent real wave packet (TDRWP) method [1] that only propagates the real part of the WP thus halving the computational effort with respect to the propagation of a complex one. This WP is then propagated by means of a Chebyshev recursion of an arccosine functional mapping of the Hamiltonian and performed a flux analysis [15] along the analysis line. We would like to highlight at this point a version CC-TDRWP that allows for the calculation of highly detailed information such as state-to-state differential cross section (DIFFREALWAVE) [16]. Both approaches share common features with the TI work of Chen and Guo [17] and of Kroes and Neuhauser, [18] and it is essentially the same as the Chebyshev real WP approach of Lin and Guo [19]. Since a finite grid is used to represent the scattering coordinates the use of absorbing potentials is necessary in order to prevent the WP reflection back into the interaction region.

From a general point of view, the TDRWP methodology allows for several procedures, depending on what kind of information is desired to obtain. Thus, the WP can be propagated in either reactant or product Jacobi coordinates and consequently analyzed by means of mainly two general methods: flux [15] or asymptotic [20] analysis methods, based in obtaining the components of either the transition or the scattering matrix, respectively. When the analysis is done in the reactant channel and through the asymptotic method, the initial wave packet is placed in the entrance channel and the analysis line is placed between the initial wave packet and the absorption region of reactants. With this setup, the inelastic event is considered and analyzed yielding all relevant inelastic state-to-state non-reactive probabilities. It is known that this approach is quite unstable numerically, especially at low energies. However, the advantage of this set up is that the part of the wave packet which moves from the interaction region into the product channel and is absorbed there is assumed to be reactive, reducing considerably the grid size and giving only information about the total reaction probability since no information about the products and products rovibrational states is obtained. If the flux based method is used the analysis line can be placed in R or r, providing the total non-reactive or the total reaction probability, respectively.

If product Jacobi coordinates are used along with the asymptotic method, the WP propagation allows obtaining directly the reaction probability, because the analysis line is located in the product channel. However, to perform the analysis in one of the product channels the WP has to be set initially in reactant coordinates and next it has to be re-expressed using the coordinates of the corresponding product channel. The whole propagation is then carried out in this product coordinates. Employing product Jacobi coordinates makes the problem technically more challenging and numerically more difficult. However, it allows computing state-to-state reaction probabilities. If the flux method is applied, the analysis surface it must be placed in the reactant channel, giving thus total non-reactive probability whereas with the surface placed in the product channel the total reaction probability is obtained.

Given the long-range nature of the interactions in the Ne + H<sub>2</sub><sup>+</sup> reactive system, large representation grids are required in the quantum dynamics simulations. This fact makes it adequate to use Jacobi reactant coordinates in the propagation and the flux method in the analysis. Therefore, it will not be possible to extract state-to-state reaction probabilities from our TDRWP calculations and these will rather come from the TI quantum scattering calculations.

The execution of a single TDRWP calculation consists of the following tasks:

- A. Set up an initial wave packet  $\psi_{\text{vib}_0}(x_0, t=0)$  in the appropriate Jacobi coordinates with the reactants in

- some particular internal rovibrational state  $(v_0, j_0)$  and a given compatible pair of values for  $J$  and  $K_0$ .
- B. Propagation of the real WP in time through the recursive Chebyshev iteration (i.e., using a shifted and scaled Hamiltonian operator).
  - C. The flux operator ( $\hat{F}$ ) is evaluated along a “slice” of the total grid at every iteration time once the propagated WP  $\psi_{v_0, j_0}(x, t)$  is expanded in TI wave functions  $\psi'_{v_0, j_0}(x, E)$  by means of a Fourier transform.
  - D. Repeat point B and C until the final propagation time is reached.
  - E. The total reaction probability for a given initial state is calculated by means of Eq. (1).

$$P_{v_0, j_0}(E) = \left\langle \psi'_{v_0, j_0}(x, E) \left| \hat{F} \right| \psi_{v_0, j_0}(x, E) \right\rangle \quad (1)$$

Due to the Coriolis coupling, the initial WP with total angular momentum BF-projection  $K_0$  will spread among all possible  $K$  values (below a given  $K_{\max}$  parameter) and these WPs will be coupled together [21]. For each  $J > 0$  as many as  $2J+1$  coupled WPs must be propagated (this is reduced to  $J$  or  $J+1$  if the parity is taken into account). The version of TDRWP code that we have employed makes use of MPI directives to distribute the computational effort among  $J+1$  (or  $K_{\max}+1$ ) processors [22].

### 3. Results

#### 3.1. Computational details

The LZHH PES [5] is an analytical many-body expansion based on the Aguado-Paniagua [23] functional form. It is derived from *ab initio* data computed using the complete active space self-consistent field (CASSCF) method and the internally contracted multireference configuration interaction (icMRCI) method with inclusion of the Davidson correction. The main feature of this PES is the presence of a potential energy well at the collinear geometry (0.54 eV deep with respect to the reactant asymptote). The well becomes shallower and a barrier rises when the Ne-H-H angle is decreased.

The parameters used for the time-independent ABC calculations are listed in Table 1. Individual reaction probabilities are converged better than 99% using these parameters, and the error is expected to be significantly smaller for more averaged quantities such as integral cross sections. As indicated in the previous section, a separate ABC calculation was carried out for each value of the total angular momentum  $J$  and the triatomic parity. Only calculations for para-hydrogen as initial reactant have been carried out.

Although partial waves up to  $J = 55$  have been included in the calculation, values of  $J$  greater than 40 have nearly no contribution to the reaction cross sections in the energy range of interest for the present study. Great care has been taken in the convergence of the maximum helicity quantum number. Test calculations have been run for a specific  $J=30$  value with  $K_{\max}=30, 25, 20, 15, 10, 0$  and no significant differences were observed for  $K_{\max} \geq 20$ . Using the parameters shown in Table 1, the maximum number of channel functions was 2123. The lowest total energy included in the calculation was 0.670 eV, which is smaller than the reaction threshold for any initial rovibrational state of the  $H_2$  molecule. Concerning the grid of energies at which calculations have been done, a particularly dense energy grid (0.4 meV) has been taken in the threshold region (0.678-0.716 eV) while the spacing has been increased to 2.6 meV for total energy values greater than 0.710 eV. Using the parameters specified in Table 1 each ABC run used approximately 400MB of RAM memory.

Table 1. Parameters employed in the ABC production runs. See Ref. [2] for details.

Parameter	value
$J_{\max}$	55
$K_{\max}$	Min(J,20)
$j_{\max}$	20
$E_{\max}$ / eV	2.3
$\rho_{\max}$ / a.u.	15.0
nsec	150

Concerning the TDRWP calculations, the parameters used in the propagations are listed in Table 2, considering  $H_2^+$  in the  $v_0=2, j_0=1$  rovibrational state and employing a symmetry adapted representation [24]. We have selected here all  $J$  values up to 7, and then  $J=10, 15, 20, 30$  for both  $K_0=0$  and 1 and  $E_{\text{col}}$  from 0.004 to 2.0 eV. Reaction probabilities were converged within  $\sim 1\%$  by propagating the initial wave packet during 80000 steps. Each thread of a CC-TDRWP job used 1600MB of memory employing the parameters listed in Table 2. The CC-TDRWP calculations are very expensive and we approximate other partial-wave probabilities via a J-shifting technique [25,26,27,28] that does not depend on the existence of a reaction barrier. In this approximation, probability thresholds are shifted with  $J$  and  $K_0$ , according to an analytically fitted expression, Eq. (2). If probabilities  $P^{J_1}$  and  $P^{J_2}$  are known and  $J \in [J_1, J_2]$ , we then estimate  $P^J$  via linear interpolation (Eq. (3)).

$$S_{j_0 K_0}^{Jp} = a_{j_0 K_0}^{Jp} J + b_{j_0 K_0}^{Jp} J^2 + c_{j_0 K_0}^{Jp} K_0^2 \quad (2)$$

$$P_{j_0 K_0}^{Jp}(E_{\text{col}}) \approx P_{j_0 K_0}^{J_1 p}(E_{\text{col}} - [S_{j_0 K_0}^{J_1 p} - S_{j_0 K_0}^{J_2 p}]) \frac{J_2 - J}{J_2 - J_1} + P_{j_0 K_0}^{J_2 p}(E_{\text{col}} + [S_{j_0 K_0}^{J_2 p} - S_{j_0 K_0}^{J_1 p}]) \frac{J - J_1}{J_2 - J_1} \quad (3)$$

Table 2. Parameters employed in the TDRWP production run. See Ref. [8] for details. Units are atomic units unless otherwise specified.

Parameter	value	Parameter	value
Scattering coordinate (R) range	0.1-20	Potential cutoff	0.44
Number of grid points in R	167	R and r absorption start at	17.0 14.0
Internal coordinate (r) range	0.5-17.0	R and r absorption strength	0.01
Number of grid points in r	153	Center and width of initial wave packet	13.5 0.15
Number of associated Legendre polynomials	100	Translational energy center of the initial WP / eV	0.70
Propagation time / fs	920 (80 000 iterations)		

### 3.2. Reaction Cross Sections

The reaction cross section of the  $Ne + H_2^+$  reaction has been calculated for the first three vibrational states of the para- $H_2^+(j_0=1)$  molecule,  $v_0=0, 1, 2$  using the CC-TDRWP and ABC codes. The results obtained by means of both methodologies are plotted in Figure 1 as a function of the collision energy. The agreement between both methods is

overall excellent, as it should be expected for two numerically converged calculations based on exact methodologies. It is however worthwhile pointing out that some discrepancies can be noticed in the region close to the reaction threshold energy. These differences are more visible in the  $v_0=2, j_0=1$  cross section and they can be explained by the difficulty of TD techniques to explore very low collision energies.

On the other hand, the ABC calculation has produced reaction cross sections for a shorter collision energy range, approximately 0.25eV. In spite of these minor differences, the main conclusion to be drawn from Figure 1 is that both methodologies fully coincide if they are appropriately converged. The choice of one technique over the other will be determined by whether one is interested in a broad range of energies or rather a specific value, in the low collision energy regime, for instance. As pointed out in the introductory section, this paper focuses on the computational performance. Thus, for the sake of brevity, we only highlight, as most relevant physical features, the strong vibrational enhancement in the reaction and the marked resonance structure in the  $v_0=2, j_0=1$  reaction cross section. Both effects have been studied in detail previously [8]. It is also worthwhile noticing that the behavior of the reaction cross section clearly changes with the reactants vibrational level. Cross sections present a threshold collision energy for  $v_0 < 2$  that practically disappears for higher vibrational states. This effect has been interpreted in terms of the late barrier character of the PES. The cross sections with threshold present a similar behavior, increasing until they reach a quasi plateau region. In the case of  $v_0=2$  cross section, this behavior is masqueraded by the more sophisticated pattern detected at low energy values.

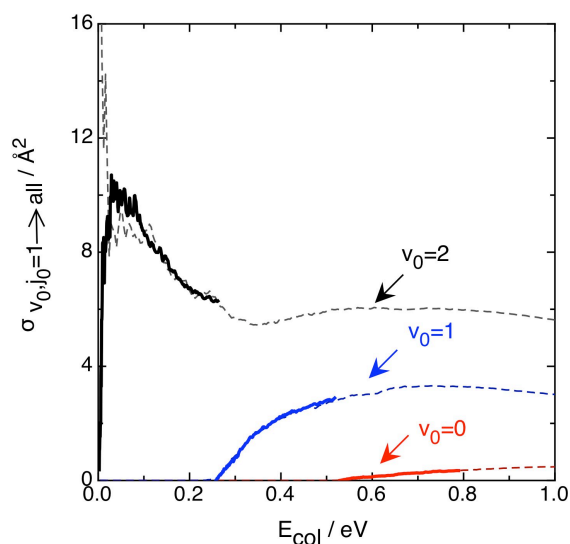


Figure 1: State-selected CC-TDRWP (light dashed line) and TI-ABC (strong solid line) reaction cross sections  $\sigma_{v_0, j_0}(E_{\text{col}})$  for  $\text{Ne} + \text{H}_2^+(v_0=0-2, j_0=1)$ . Red, blue and black lines stand for initial vibrational levels  $v_0=0, 1$  and  $2$ , respectively.

### 3.3. Computational performance of CC-TDRWP and ABC

The comparable accuracy of TD and TI quantum scattering approaches, which was just proven for the title system, has been acknowledged for some time in the reaction dynamics community [29]. Let us thus focus our attention rather on the computational effort associated to the calculations. In order to produce the data shown in Figure 1 using the TD approach, a specific simulation needed to be carried out for each of the three initial reactant states ( $v_0=0,1,2$  and  $j_0=1$ ). Given that the rotational  $j_0=1$  state has three compatible values of the quantum number

associated to its projection on the quantization axis (helicity quantum number,  $K$ ) the CC-TDRWP calculations are actually three for each state ( $v_0, j_0=1, K_0=0, \pm 1$ ). On the other hand, being the reactant molecule  $\text{H}_2^+$  homonuclear one can safely assume that the same reaction probability will be obtained for a  $K_0=+1$  and a  $K_0=-1$  calculation. Therefore, in order to produce the results shown in Figure 1 using the CC-TDRWP method we have run 6 wave packet propagations for each value of the total angular momentum explicitly considered. Considering that we have estimated a value of  $J_{\text{max}}=55$  to obtain numerically converged results and that only the  $K_0=0$  value is compatible with  $J=0$ , the computational campaign to generate Figure 1 would imply a total of 333 CC-TDRWP calculations. The cost of each individual calculation critically depends on  $K_{\text{max}}$  since the Coriolis term in the Hamiltonian couples different  $K$  values as mentioned previously in the methodology section. Moreover, as it has been explained in the previous section, only some selected  $J$  values have been calculated and a  $J$ -interpolation scheme has been applied.

The time-independent ABC code yields the full state-to-state scattering matrix and therefore one single calculation is enough to produce reaction probabilities for all three rovibrational states of the  $\text{H}_2^+$  molecule. Two calculations need to be performed for each value of the total angular momentum for both possible values of the triatomic parity. Thus, to obtain the three excitation functions shown in Figure 1 the TI ABC needs to be executed 111 times (only the even parity is compatible with  $J=0$ ). In the case of the TI calculation we have indeed carried out explicitly the calculations for all values of  $J$  between 0 and 55. The crude comparison between the number of TD and TI calculations is however misleading. The formal resolution of the reactive scattering problem using a TI strategy produces the full scattering matrix but restricted to a given value of the total energy. This would mean that a simple minded application of a TI method would require of 111 calculation for each point in the curves. The ABC code was cleverly designed to avoid such an inefficient strategy and makes use of the fact that steps A and B (see Section 2) are independent of the total energy (below a given value  $E_{\text{max}}$ ) and only steps C to D need to be repeated. The computational effort of each ABC calculation thus depends on the  $K_{\text{max}}$  value, already pointed out in the CC-TDRWP case, and the density of the energy grid.

As it has been pointed out previously, probably the most critical parameter to be converged, from the computational cost point of view is the maximum value of the total angular momentum projection,  $K_{\text{max}}$ . In order to illustrate this, Figure 2 shows the CPU time consumed in getting the TI and TD cross sections for a value of the total angular momentum  $J=30$ . Both calculations are run on the same infrastructure, a cluster of two [dual] six core Intel Xeon X5650 at 2.66 GHz nodes connected by Infiniband QDR 4X. Although the total CPU consumed time is accounted for in Figure 2, the CC-TDRWP code benefits from MPI parallelization and the  $K_{\text{max}}=30$  calculation was distributed among 31 cores. Obviously, the comparison may not be done straightforwardly, so some considerations have been taken into account. In order to make the comparison in the same conditions, and since the number of discrete energy values of TD cross sections plotted in Figure 1 is 500, this is concretely the total number of individual TI calculations performed. As mentioned above the CC-TDRWP propagation needs to be repeated for each value of  $K_0=0, 1$  and  $v_0=0, 1, 2$  (the TD curve in Figure 2 corresponds to the  $v_0=2, j_0=1, K_0=1$  calculation), while the TI-ABC requires the calculation of the even and odd parities (the TI curve in Figure 2 corresponds to the even calculation). Moreover, another sink of time is the number of rotational basis set used (Legendre polynomials). In particular, CC-TDRWP execution time has been scaled in order to use the same number of basis set as the ABC method. According to Table 2, TD propagations have used 50 Legendre polynomials whereas only 20 functions were used in the TI code. Some checks have evidenced that the time consumed is reduced in a half so this factor has been applied to the CC-TDRWP CPU time consumed. The last consideration is that we have estimated the time needed to perform all the propagations at each  $J$  value until 30 since in the TD procedure only propagations at selected  $J$  values were performed, obtaining the rest of probabilities by means of the  $J$ -shifting technique described in the computational details section. Taken all these considerations into account, a similar CPU time is consumed for each of the methods compared. In the case of CC-TDRWP method a total of 6730 CPU hours are consumed for a single  $K_0=1$  projection using the MPI parallel code whereas a total of 6890 CPU hours are needed in the case of



time-independent ABC code.

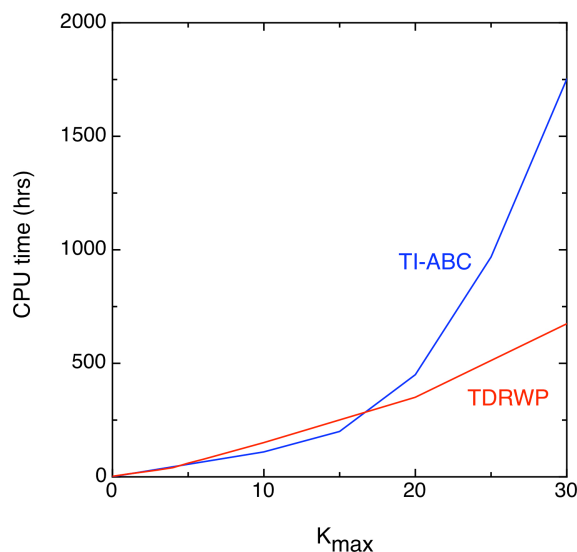


Figure 2: CPU time used in the computation of a single partial wave calculation as a function of the total angular momentum projection,  $K_{\max}$ . The TI-ABC CPU time has been obtained by estimating a single calculation with 500 energy values.

The CPU time curves plotted in Figure 2 illustrate how the computational effort in the calculation critically depends on the maximum helicity quantum number, the  $K_{\max}$  parameter. This increase in both TD and TI calculations is mainly due to the evaluation of the Coriolis term in the accurate Hamiltonian. The Coriolis term couples wave packets in the TD approach (basis functions in the TI one) associated to a quantum number  $K$  with those with quantum number  $K \pm 1$ . The increase is especially dramatic in the case of the TI-ABC program when the CPU time is doubled with respect to the TDRWP for  $K_{\max} \geq 20$ . On the other hand, this scenario reverses its tendency for  $K_{\max} \leq 20$  where the ABC method manages more efficiently this number of coupled  $K$  values than the CC-TDRWP method.

#### 4. Conclusions

The Reaction Dynamics community possesses two highly competitive tools for the accurate quantum simulation of elementary reactions. To our judgment, it cannot be straightforwardly stated whether time-dependent strategies offer more advantages rather than time-independent ones. These techniques are rather complementary in our view, offering a continuous range of energies in the case of TD (depending on the initial WP) and the full scattering matrix in the case of TI. While it can be claimed that the WP approach encounters some difficulties propagating initial wave packets with very low collision energies, it might also be argued that it leads to an easier interpretation of the microscopic mechanism of the reaction. That is to say, it leads to a clearer (intuitive) picture of what happens when a reactive collision occurs. Numerically, it cannot be firmly stated whether TD approaches is computationally more efficient than TI, or vice versa. In both cases, the critical factor determining the cost of an accurate simulation is the maximum value of the helicity quantum number,  $K_{\max}$ . This increase is particularly dramatic in the case of reaction with large potential energy wells where the insertion mechanism is clearly dominant and all helicity quantum numbers need to be considered, i.e.  $K_{\max} = J$  [30, 31]. In the case of the  $\text{Ne} + \text{H}_2^+ \rightarrow \text{NeH}^+ + \text{H}$  reaction the ABC code scaled worse in the evaluation of the Coriolis coupling for values of  $K$  higher than 20, whereas the method was faster than TDRWP for lower values. The conclusions of our study are, for the time being, restricted to triatomic reactions given that no TI quantum scattering code for higher dimensionality reactions has been made available for

its general straightforward use.

## **Acknowledgements**

This work was supported by the Spanish Ministry of Science and Innovation (MICINN projects CTQ2011-27857-C02-01 and CTQ2009-12215/BQU). Thanks are also given to the “Generalitat de Catalunya” (Autonomous Government of Catalonia, ref. 2009SGR 17 and Xarxa de Referència en Química Teòrica i Computacional de Catalunya (XRQTC)).

## **References**

- [1] S. K. Gray, G. G. Balint-Kurti, *J. Chem. Phys.*, 108, 950 (1998).
- [2] D. Skouteris, J. F. Castillo, D. E. Manolopoulos *Comp. Phys. Comm.*, 133, 128 (2000).
- [3] A. Laganà, A. Riganeli, Eds., “Reaction and Molecular Dynamics, Lecture Notes in Chemistry, V.75, Springer, Berlin, Germany (2000).
- [4] R. D. Levine, “Molecular Reaction Dynamics”, Cambridge University Press, UK, 2005.
- [5] S. J. Lv, P. –Y. Zhang, K. L. Han, G. –Z. He, *J. Chem. Phys.*, 132, 014303 (2010).
- [6] F. Huarte-Larrañaga, X. Giménez, J. M. Lucas, A. Aguilar, J.-M. Launay, *Phys. Chem. Chem. Phys.*, 1, 1125 (1999).
- [7] F. Huarte-Larrañaga, X. Giménez, J. M. Lucas, A. Aguilar, J.-M. Launay, *J. Phys. Chem. A* 104, 10227 (2000).
- [8] P. Gamallo, P. Defazio, M. González, *J. Phys. Chem. A* 115, 11525 (2011).
- [9] P. Pendergast, J. M. Heck, E. F. Hayes, R. Jaquet, *J. Chem. Phys.*, 98, 4543 (1993).
- [10] C. Petrongolo, *J. Chem. Phys.*, 89, 1297 (1988).
- [11] G. C. Schatz, *Chem. Phys. Lett.*, 150, 92 (1988).
- [12] F. Huarte-Larrañaga, X. Giménez, A. Aguilar, M. Baer, *Chem. Phys. Lett.*, 291, 346 (1998).
- [13] D. E. Manolopoulos, *J. Chem. Phys.*, 85, 6425 (1986).
- [14] R. T. Pack, G. A. Parker, *J. Chem. Phys.*, 87, 3888 (1987).
- [15] J. H. M. Meijer, E. M. Goldfield, S. K. Gray, G. G. Balint-Kurti, *Chem. Phys. Lett.*, 293, 270 (1998).
- [16] M. Hankel, S.C. Smith, S. K. Gray, G. G. Balint-Kurti, *Comp. Phys. Comm.*, 179, 569 (2008)
- [17] R. Chen, H. Guo, *J. Chem. Phys.*, 105, 3569 (1996).
- [18] G.-J. Kroes, D. Neuhauser, *J. Chem. Phys.*, 105, 8690 (1996).
- [19] S. Y. Lin, H. Guo, *Phys. Rev. A* 74, 022703 (2006).
- [20] G. G. Balint Kurti, R. N. Dixon, C. C. Marston, *J. Chem. Soc., Faraday Trans.* 86, 1741 (1990).
- [21] P. Defazio, P. Petrongolo, *J. Chem. Phys.* 127, 204311 (2007).
- [22] C. Petrongolo, P. Defazio, unpublished work.
- [23] A. Aguado, M. Paniagua, *J. Chem. Phys.*, 96, 1265 (1992).
- [24] P. Defazio, B. Bussery-Honvault, P. Honvault, C. Petrongolo, *J. Chem. Phys.*, 135, 114308 (2011).
- [25] J. M. Bowman, *J. Phys. Chem.* 95, 4960 (1991).
- [26] S. K. Gray, G. G. Balint Kurti, G. C. Schatz, J. J. Lin, X. Liu, S. Harich, X. Jang, *J. Chem. Phys.*, 113, 7330 (2000).
- [27] I. Miquel, M. González, R. Sayós, G. G. Balint Kurti, S. K. Gray, E. M. Goldfield, *J. Chem. Phys.*, 118, 3111 (2003).
- [28] P. Gamallo, P. Defazio, M. González, C. Petrongolo, *J. Chem. Phys.*, 129, 244307 (2008).
- [29] S. C. Althorpe, D. C. Clary, *Ann. Rev. Chem.*, 54, 493 (2003).
- [30] N. Balucani, G. Capozza, L. Cartechini, A. Bergeat, R. Bobbenkamp, P. Casavecchia, F.J. Aoiz, L. Bañares, P. Honvault, B. Bussery-Honvault, J.M. Launay, *Phys. Chem. Chem. Phys.*, 6, 4957 (2004).
- [31] T. González-Lezana, *Int. Revs. in Phys. Chem.*, 26, 29 (2007).